Modern Journal of Statistics
1(1), 80–103
DOI: https://doi.org/10.64389/mjs.2025.01112
https://sphinxsp.org/journal/index.php/mjs

Research article

Development and Applications of a New Hybrid Weibull-Inverse Weibull Distribution

Nooruldeen A. Noori[1*], Kamal Najim Abdullah[2], and Mundher A. khaleel[2]

[1]Anbar Education Directorate, Anbar 31002, Iraq; Nooruldeen.a.noori35508@st.tu.edu.iq

[2]Mathematics Departments, College of Computer Science and Mathematics, Tikrit University, Tikrit 34001, Iraq; Kn230022pcm@st.tu.edu.iq, mun880088@tu.edu.iq

***Correspondence:** Nooruldeen.a.noori35508@st.tu.edu.iq

ARTICLE INFO

Keywords:
Weibull distribution
Parameter estimation
Hybrid distributions
Monte-Carlo simulation
Real data analysis

Mathematics Subject Classification:
62F10, 62P10

Important Dates:
Received: 8 June 2025
Revised: 8 July 2025
Accepted: 10 July 2025
Online: 12 July 2025

ABSTRACT

This study introduces and applies a novel statistical model known as the hybrid Weibull inverse Weibull (HWIW) distribution, which combines the characteristics of the Weibull and inverse Weibull distributions to provide a more flexible model for representing real-world data, especially those characterized by asymmetry or extreme values. The basic functions of the distribution were derived, along with other statistical measures such as moments, the quantile function, and entropy were also derived. The distribution parameters were estimated using three distinct approaches, and their performance was evaluated through a Monte Carlo simulation to assess the performance and precision of each estimation technique. The results were used to show the most accurate estimation method for different samples. The proposed model was utilized to test two practical datasets; the findings demonstrated that the HWIW distribution outperformed six competing IW distributions in terms of model selection metrics. These results confirm the efficiency of the HWIW model's ability to capture the structure of complex datasets and open the way for its use in multiple applications, including medical, industrial, and social fields, with the potential to be expanded to include multidimensional data or integrated with artificial intelligence techniques.

1. Introduction

Probability distribution plays a fundamental role in the field of statistical modeling and data analysis. They are the primary tool for understanding the random behavior associated with various scientific and applied phenomena, from reliability analysis and forecasting to risk assessment and statistical engineering. Among the common distribution, the Weibull distribution stands out for its high flexibility in representing failure and reliability data, while the inverse Weibull distribution is characterized by its ability to represent data characterized by non-constant failure rates or heterogeneous behavior. Despite the representative power of each of these two distributions individually, using either of them alone may not be sufficient to represent real-world data characterized by asymmetry, heavy tails, or high levels of dispersion. This often leads to poor estimation accuracy and poor fit of statistical models.

This challenge has prompted researchers to search for more flexible statistical alternatives that go beyond the limitations imposed by traditional models. Hence, the idea of hybrid distributions arose, which aims to combine the characteristics of two or more distribution within a single statistical model, giving the model greater adaptability to diverse data characteristics. Recent developments in this field have contributed to the emergence of the T-X methodology, one of the most prominent methods used to generate new distribution by transforming basic distribution using flexible transformation functions. This methodology has resulted in the emergence of several new distribution families [1], such as BIIIEE-X family [2], NOGEE−G family [3], WEE-X Family[2], OLG family [5], NGOF-G Family [6], EOIW-G Family [7], GOM-G family [8], HOLGE [9], and HOE-Φ family [10], which have proven effective in representing non-standard data with heterogeneous properties.

This research presents a new distribution model within the framework of the HWG family, which relies on transforming basic distribution into more flexible distribution. This family has a CDF of the form [11] :

$$F_{HWG}(x,r,u,\xi) = 1 - e^{\left(-r\left[-\Psi(x;\varepsilon).log\left(1-\Psi(x;\varepsilon)\right)\right]^{u}\right)}, \qquad x \geq 0, r, u > 0. \tag{1.1}$$

While its PDF takes the form:

$$f_{HWG}(x,r,u,\xi) = ru\,\psi(x;\varepsilon)\left[\frac{\Psi(x;\varepsilon)}{1-\Psi(x;\varepsilon)} - log\left(1-\Psi(x;\varepsilon)\right)\right]$$
$$\times\left[-\Psi(x;\varepsilon).log\left(1-\Psi(x;\varepsilon)\right)\right]^{u-1} e^{\left(-r\left[-\Psi(x;\varepsilon).log\left(1-\Psi(x,\varepsilon)\right)\right]^{u}\right)}, \tag{2.1}$$

where $\Psi(x;\varepsilon)$ and $\psi(x;\varepsilon)$ represent the CDF and PDF functions, the paramters r and u characterize the shape of the HWG family, based on any specified base distribution, such that $r, u \geq 0$.

Although probability distributions are widely used in statistical modeling and data analysis, traditional distributions often face challenges in accurately representing complex data, especially those that are asymmetric or contain extreme values. With advances in statistical methods, there is a growing need to develop more flexible models capable of effectively handling such data. Among the commonly used distribution, the Weibull and inverse Weibull distribution are important; however, when applied individually, they may not always yield sufficiently accurate or satisfactory results. A review of the literature reveals a lack of studies that integrate these two distributions into a single model that leverages the strengths of both.

Accordingly, a new statistical distribution is presented in this work called the HWIW distribution, characterized by high flexibility and improved capability in representing real-world data. This study includes deriving examining the statistical characteristics of the proposed distribution and determining its parameters through three distinct estimation techniques: MLE, LSE, WLSE. Its performance is then evaluated by applying the model to real dataset and comparing it with several other distributions to assess its accuracy and efficiency.

This paper is organized as follows. In Section 2, we derived other proposed model main functions. The statistical properties of the HWIW distribution were calculated in Section 3. Estimators of the proposed model were presented in Section 4 by three different methods, and the simulation in Section 5 was used to check these methods' behavior. Section 6 used two practical datasets to show the HWIW distribution superiority for fitting them. Finally, concluding remarks for the whole paper were written in Section 7.

2. The hybrid Weibull inverse Weibull (HWIW) distribution

We assume that the underlying distribution follows the IW distribution, where the PDF and CDF can be represented as follows [12]:

$$\Psi(x;b,c) = e^{-bx^{-c}} \quad , b, c, x > 0, \tag{2.1}$$

$$\psi(x;q,p) = bcx^{-(c+1)}e^{-bx^{-c}} \quad ,b,c,x > 0, \tag{2.2}$$

where b, c are shape parameters for IW distribution.

In order the obtain the CDF of the HWIW distribution, Equation (1.1) and (3) are combined into a unified from as follows:

$$F(x) = 1 - e^{\left(-r\left[-e^{-bx^{-c}}.log\left(1-e^{-bx^{-c}}\right)\right]^{u}\right)}, \qquad x\, r, u, b, c > 0. \tag{2.3}$$

Substituting Equation (2.1) into Equation (2.1) and 4, the PDF of the HWIW distribution can be expresses as:

$$f(x) = rubcx^{-(c+1)}e^{-bx^{-c}}\left[\frac{e^{-bx^{-c}}}{1-e^{-bx^{-}}} - log\left(1 - e^{-bx^{-c}}\right)\right]\left[-e^{-bx^{-c}}.log\left(1 - e^{-bx^{-c}}\right)\right]^{u-1} e^{\left(-r\left[-e^{-bx^{-c}}.log\left(1-e^{-bx^{-c}}\right)\right]^{u}\right)}. \tag{2.4}$$

Figures 1 and 2 illustrate the PDF and CDF of the HWIW distribution under various parameter settings. As depicted in Figure 1, the PDF curves demonstrate a wide variety of shapes, including decreasing trends, unimodal peaks, right-skewed forms, and reverse J-shapes. This diversity highlights the distribution's high flexibility and its ability to model different types of data, especially those with asymmetric behavior or heavy tails.

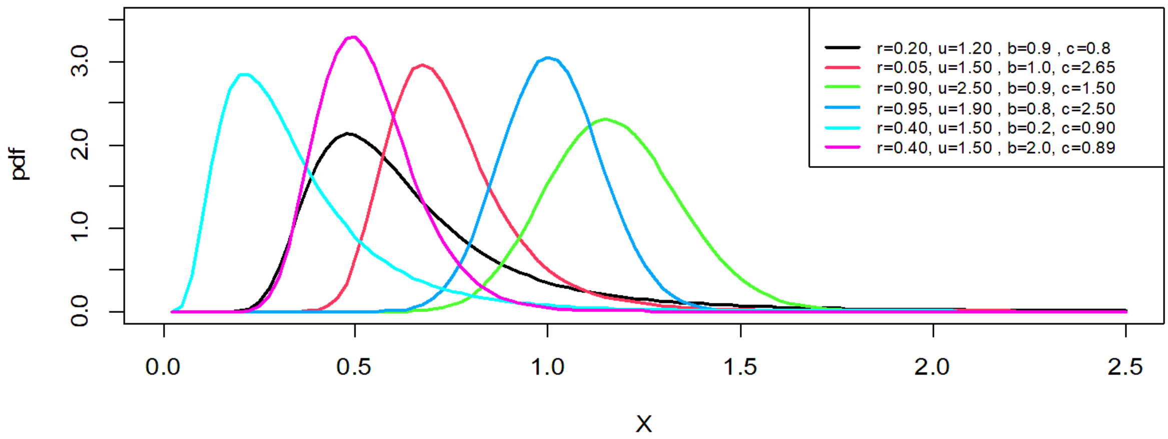

Figure 1: PDF curves of the HWIW distribution under varying parameter values.

Figure 2 presents the CDF curves, which all start from zero and asymptotically approach one, as expected. The variation in the steepness of the curves reflects the adaptability of the distribution to different accumulation patterns of probability. All graphs were generated using the R programming language, emphasizing the statistical rigor and visual clarity of the analysis.
The survival function corresponding to the HWIW distribution is given by the following expression [13] :

$$S(x) = e^{\left(-r\left[-e^{-bx^{-c}}.log\left(1-e^{-bx^{-c}}\right)\right]^{u}\right)}. \tag{2.5}$$

The hazard function associated with the HWIW distribution is mathematically formulated as follows [14]:

$$h(x) = rubcx^{-(c+1)}e^{-bx^{-c}}\left[\frac{e^{-bx^{-c}}}{1-e^{-bx^{-}}} - log\left(1 - e^{-bx^{-c}}\right)\right]\left[-e^{-bx^{-c}}.log\left(1 - e^{-bx^{-c}}\right)\right]^{u-1}. \tag{2.6}$$

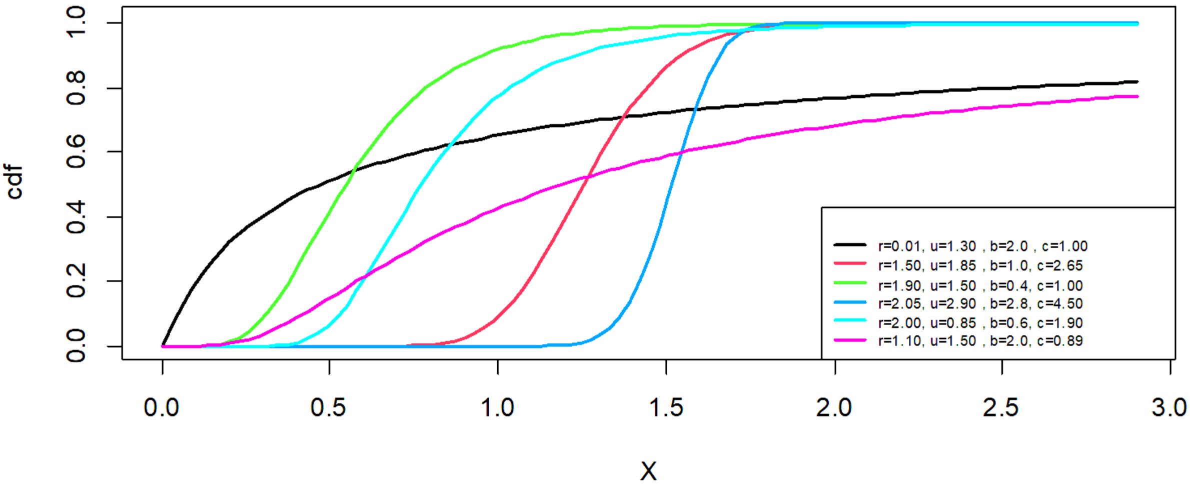

Figure 2: CDF curves of the HWIW distribution under varying parameter values.

Figures 3 and 4 highlight the behavior of both survival and hazard curves for the HWIW distribution given different parameters (r, u, b, c) highlighting its flexibility in representing various failure patterns. In Figure 3, the survival functions $S(x)$ gradually decrease from 1 as x increases, with some curves indicating early failure (e.g., green), while others reflect longer survival (e.g., purple and black).

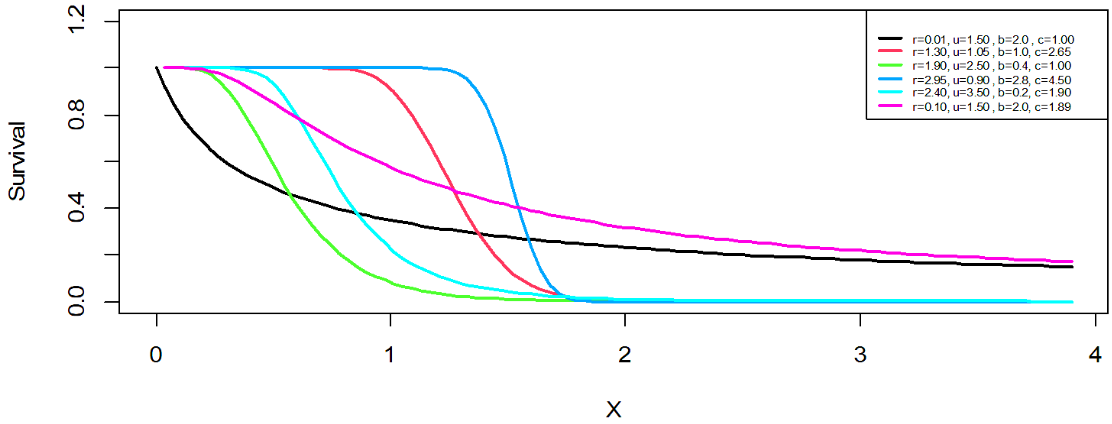

Figure 3: Survival curve plot of the HWIW distribution.

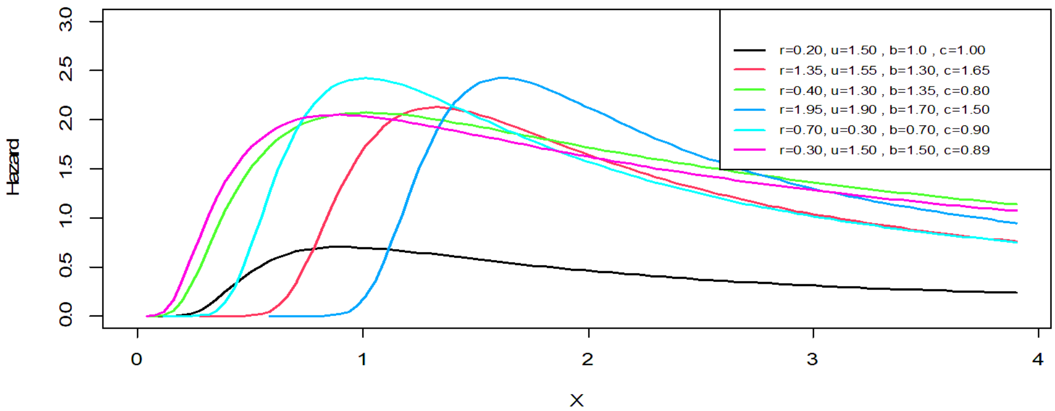

Figure 4: hazard curve plot of the HWIW distribution.

Figure 4 highlights the diversity in the pattern of the hazard function $h(x)$. Some curves exhibit a decreasing pattern indicating aging, while others adopt a non-monotonic shape that begins with a rise, then decreases, then increases, resembling the shape of a bathtub familiar from reliability analysis.

Due to the complexity of the original formulas for the CDF and PDF in Equations (5) and (6), we simplified them to facilitate the derivation of the dividends for the HWIW distribution. This was done by applying expansions such as the utilizing the series forms of binomial, the exponential, and logarithm expansion, resulting in a formula for the CDF as follows:

$$F(x) = 1 - \varphi\left(e^{-bx^{-c}}\right)^{j+2iu}, \tag{2.7}$$

where $\varphi = \sum_{i=j=0}^{\infty} \frac{(-1)^{i+iu+j}}{i!} r^i d_{iu,j}$, and $d_{iu,j} = j^{-1} \sum_{m=1}^{j} \frac{m(iu+1)-j}{m+1} \quad for\ j \geq 0\ and\ d_{iu,0} = 1$.

Following the same approach, the PDF can also be simplified through mathematical expansion, leading to the following formula:

$$f(x_N) = \mathrm{M}x^{-(c+1)}\mathrm{e}^{-(2iu+2u+j+k)bx^{-c}} - Nx^{-(c+1)}\mathrm{e}^{-(2iu+2u+j+z)bx^{-c}}, \tag{2.8}$$

where $M = \sum_{i=j=k=0}^{\infty} \frac{(-1)^{i+iu+u-1+j+k}}{i!} r^{i+1} d_{iu+u-1,j}\, u\, bc$, and $N = \sum_{i=j=z=0}^{\infty} \frac{(-1)^{i+iu+u-1+j+z}}{i!} r^{i+1} d_{iu+u-1,j}$.

As $d_{1,z} = z^{-1} \sum_{m=1}^{j} \frac{2m-j}{m+1} \quad for\ z \geq 0 \quad and\ d_{1,0} = 1$ and $d_{iu+u-1,j} = j^{-1} \sum_{m=1}^{j} \frac{m(iu+u)-j}{m+1} \quad for\ j \geq 0 \quad and\ d_{iu+u-1,0} = 1$.

3. Properties for HWIW distribution

3.1 Quantile function for HWIW distribution

Theorem: If $F(x)$ represents the CDF of the HWIW distribution, such that $F(x): \mathbb{R} \to [0,1]$ is an increasing, non-decreasing function, then the corresponding quantile function $Q(p)$ for this distribution is given by:

$$Q(p) = \left[\frac{ log \left[\frac{ \left[\frac{-\,log(1-p)}{r} \right]^{\frac{1}{u}} }{ \left[\frac{-\,log(1-p)}{r} \right]^{\frac{1}{u}} + W_{-1} \left[\frac{-\,log(1-p)}{r} \right]^{\frac{1}{u}} e^{-\left[\frac{-\,log(1-p)}{r} \right]^{\frac{1}{u}}} } \right] }{b} \right]^{\frac{-1}{c}}. \tag{3.1}$$

Proof: let $p = F(x)$ be the CDF of the HWIW distribution

Assume that $z = e^{-bx^{-c}}$, then $p = 1 - e^{(-r[-Z.\ log(1-Z)]^u)} \Longrightarrow 1 - p_N = e^{(-r[-Z.\ log(1-Z)]^u)}$. Take the log for both sides to get: $\log(1-p) = -r[-Z.\ log(1-Z)]^u$. We divide both sides by $-r$, so we get: $\frac{-\,log(1-p)}{r} = [-z.log(1-z)]^u$. Take raise both sides to strength $(\frac{1}{u})$ to get: $\left[\frac{-\,log(1-p)}{r}\right]^{\frac{1}{u}} = -z.\log(1-z)$. Multiply both sides of the equation by -1 we get:$-\left[\frac{-\,log(1-p)}{r}\right]^{\frac{1}{u}} = z.\log(1-z)$.

To simplify the expression, we define a substitution variable v as follows: $v = -\left[\frac{-\log(1-p)}{r}\right]^{\frac{1}{u}}$.

So that $z.\log(1-z) = v \Rightarrow \log(1-z) = \frac{v}{z}$.

$$\text{let } \theta = \frac{v}{z} \Rightarrow z = \frac{v}{\theta} \Rightarrow 1 - z = 1 - \frac{v}{\theta} = \frac{\theta - v}{\theta},$$

$$\log\left(\frac{\theta - v}{\theta}\right) = \theta \Rightarrow \frac{\theta - v}{\theta} \Rightarrow \theta = v + W_{-1} v e^{-v},$$

where the W_{-1} is the lower branch of the lambert W function [5] then: $z = \frac{v}{v + W_{-1} v e^{-v}}$.

Now, substitute back to find x: $e^{-bx^{-c}} = \frac{v}{v + W_{-1} v e^{-v}}$, take the log for both sides to get: $-bx^{-c} = \log\left[\frac{v}{v + W_{-1} v e^{-v}}\right]$.

Dividing both sides by $-$b yields: $x^{-c} = \frac{\log\left[\frac{v}{v + W_{-1} v e^{-v}}\right]}{-b}$, take raise both sides to strength $(-\frac{1}{c})$ to get: $x = \left[\frac{\log\left[\frac{v}{v + W_{-1} v e^{-v}}\right]}{-b}\right]^{\frac{-1}{c}}$.

Finally, using the original definition of v, the quantile function Q(p) is:

$$Q(p) = \left[\frac{\log\left[\frac{\left[\frac{-\log(1-p)}{r}\right]^{\frac{1}{u}}}{\left[\left[\frac{-\log(1-p)}{r}\right]^{\frac{1}{u}} + W_{-1}\left[\frac{-\log(1-p)}{r}\right]^{\frac{1}{u}} e^{-\left[\frac{-\log(1-p)}{r}\right]^{\frac{1}{u}}}\right]}\right]}{b}\right]^{\frac{-1}{c}}$$

Finally, we get a form in Equation (3.1).

A numerical representation of our proposed model quantile function is determined in Table 1.

Table 1: Quintile function of HWIW distribution.

q	(r, u, b, c)				
	(0.7,1.3,0.4,0.2)	(0.6,1.5,1.4,1)	(0.5,1.1,0.9,1.1)	(1.2,1,0.8,1.2)	(0.7,1.9,0.7,0.5)
0.1	0.0218168	1.906395	1.062304	0.6697021	1.099829
0.2	0.1115255	2.620930	1.532390	0.8610302	1.868169
0.3	0.3981566	3.348908	2.071615	1.0475163	2.765094
0.4	1.2719911	4.176776	2.766355	1.2531876	3.890400
0.5	4.0414550	5.189129	3.744756	1.4990069	5.381479

0.6	13.8737973	6.519626	5.267047	1.8168022	7.483554
0.7	57.2273272	8.437554	7.985730	2.2706451	10.714995
0.8	347.7596965	11.637871	14.089895	3.0296305	16.449317
0.9	574.1890165	18.902468	36.712721	4.8052371	30.300980

3.2 Moment function for HWIW distribution

Theorem: let X be a random variable governed by HWIW distribution and $f(x)$ represents its pdf, then the moment of order n for this distribution is given by:

$$\mu_n = \frac{\Gamma\left(\frac{n-c}{c}\right)}{cb^{\frac{n-c}{c}}}\left[\frac{M}{(2iu+2u+j+k)^{\frac{n-c}{c}}} - \frac{N}{(2iu+2u+j+z)^{\frac{n-c}{c}}}\right]. \quad (3.2)$$

Proof: assume X is a random variable with pdf is $f(x)$, then the moment of order n is then given by the following expression [15], [9] :

$$\mu_n = E(x^n)_{HWIW} = \int_0^\infty x^n f_{HWIW}(x)dx,$$

substituting Equation (2.8) into the previous expression yields the following result

$$\mu_n = \int_0^\infty x^n \left(\mathrm{M}x^{-(\mathrm{c}+1)}\mathrm{e}^{-(2\mathrm{iu}+2\mathrm{u}+\mathrm{j}+\mathrm{k})bx^{-c}} - Nx^{-(\mathrm{c}+1)}\mathrm{e}^{-(2\mathrm{iu}+2\mathrm{u}+\mathrm{j}+\mathrm{z})bx^{-c}}\right)dx,$$

$$\mu_n = M\int_0^\infty x^{n-(\mathrm{c}+1)}\,\mathrm{e}^{-(2\mathrm{iu}+2\mathrm{u}+\mathrm{j}+\mathrm{k})bx^{-c}}dx - N\int_0^\infty x^{\mathrm{n}-(\mathrm{c}+1)}\mathrm{e}^{-(2\mathrm{iu}+2\mathrm{u}+\mathrm{j}+\mathrm{z})bx^{-c}}dx,$$

$$\mu_n = MI_1 - NI_2,$$

where $I_1 = \int_0^\infty x^{n-(\mathrm{c}+1)}\,\mathrm{e}^{-(2\mathrm{iu}+2\mathrm{u}+\mathrm{j}+\mathrm{k})bx^{-c}}dx$, and $I_2 = \int_0^\infty x^{\mathrm{n}-(\mathrm{c}+1)}\mathrm{e}^{-(2\mathrm{iu}+2\mathrm{u}+\mathrm{j}+\mathrm{z})bx^{-c}}dx.$

For I_1, let $y = (2\mathrm{iu}+2\mathrm{u}+\mathrm{j}+\mathrm{k})bx^{-c}$

$$x = \frac{y^{\frac{1}{c}}}{b^{\frac{1}{c}}(2\mathrm{iu}+2\mathrm{u}+\mathrm{j}+\mathrm{k})^{\frac{1}{c}}} \Rightarrow dx = \frac{\frac{1}{c}y^{\frac{1}{c}-1}}{b^{\frac{1}{c}}(2iu+2u+j+k)^{\frac{1}{c}}}dy.$$

Then $I_1 = \int_0^\infty \left(\frac{y^{\frac{1}{c}}}{b^{\frac{1}{c}}(2iu+2u+j+k)^{\frac{1}{c}}}\right)^{n-(c+1)} e^{-y}\frac{\frac{1}{c}y^{\frac{1}{c}-1}}{b^{\frac{1}{c}}(2iu+2u+j+k)^{\frac{1}{c}}}dy$, simplify I_1 to obtain the following final from:

$$I_1 = \frac{1}{cb^{\frac{n-c}{c}}(2iu+2u+j+k)^{\frac{n-c}{c}}}\int_0^\infty y^{\frac{n-c}{c}-1}e^{-y}dy,$$

$$I_1 = \frac{\Gamma\left(\frac{n-c}{c}\right)}{cb^{\frac{n-c}{c}}(2iu+2u+j+k)^{\frac{n-c}{c}}}.$$

Following a similar procedure for I_2 , we arrive at the final form

$$I_2 = \frac{\Gamma\left(\frac{n-c}{c}\right)}{cb^{\frac{n-c}{c}}(2iu+2u+j+z)^{\frac{n-c}{c}}},$$

Finally, we get a from in Equation (3.2).

The first four moments are derived by substituting different values of n, as shown below:

$$\mu_1 = \frac{\Gamma\left(\frac{1-c}{c} -\right)}{cb^{\frac{1-c}{c}}}\left[\frac{M}{(2iu+2u+j+k)^{\frac{1-c}{c}}} - \frac{N}{(2iu+2u+j+z)^{\frac{1-c}{c}}}\right],$$

$$\mu_2 = \frac{\Gamma\left(\frac{2-c}{c} -\right)}{cb^{\frac{2-c}{c}}}\left[\frac{M}{(2iu+2u+j+k)^{\frac{2-c}{c}}} - \frac{N}{(2iu+2u+j+z)^{\frac{2-c}{c}}}\right],$$

$$\mu_3 = \frac{\Gamma\left(\frac{3-c}{c} -\right)}{cb^{\frac{3-c}{c}}}\left[\frac{M}{(2iu+2u+j+k)^{\frac{3-c}{c}}} - \frac{N}{(2iu+2u+j+z)^{\frac{3-c}{c}}}\right],$$

$$\mu_4 = \frac{\Gamma\left(\frac{4-c}{c} -\right)}{cb^{\frac{4-c}{c}}}\left[\frac{M}{(2iu+2u+j+k)^{\frac{4-c}{c}}} - \frac{N}{(2iu+2u+j+z)^{\frac{4-c}{c}}}\right].$$

Using this result, we obtain the skewness and kurtosis for the HWIW distribution in the following manner:

$$SK_{HWIW} = \frac{\frac{\Gamma\left(\frac{3-c}{c} -\right)}{cb^{\frac{3-c}{c}}}\left[\frac{M}{(2iu+2u+j+k)^{\frac{3-c}{c}}} - \frac{N}{(2iu+2u+j+z)^{\frac{3-c}{c}}}\right]}{\left(\frac{\Gamma\left(\frac{2-c}{c} -\right)}{cb^{\frac{2-c}{c}}}\left[\frac{M}{(2iu+2u+j+k)^{\frac{2-c}{c}}} - \frac{N}{(2iu+2u+j+z)^{\frac{2-c}{c}}}\right]\right)^{\frac{3}{2}}},$$

$$KU_{HWIW} = \frac{\frac{\Gamma\left(\frac{4-c}{c} -\right)}{cb^{\frac{4-c}{c}}}\left[\frac{M}{(2iu+2u+j+k)^{\frac{4-c}{c}}} - \frac{N}{(2iu+2u+j+z)^{\frac{4-c}{c}}}\right]}{\left(\frac{\Gamma\left(\frac{2-c}{c} -\right)}{cb^{\frac{2-c}{c}}}\left[\frac{M}{(2iu+2u+j+k)^{\frac{2-c}{c}}} - \frac{N}{(2iu+2u+j+z)^{\frac{2-c}{c}}}\right]\right)^{2}} - 3.$$

Table 2 displays the intervals of some moments of the HWIW distribution, illustrating how these moments change as the distribution's parameters change. It also highlights the effect of the parameters on the first four moments, which helps analyze the distribution's statistical properties when parameter values vary.

Table 2: displays the intervals of some moments of the HWIW distribution.

r	u	b	c	μ_1	μ_2	μ_3	μ_4	$Var(X)$	skew	kurtosis
0.8	1.6	0.4	1.1	1.596876	4.786326	37.61691	1363.256	2.236313	3.592359	59.50766
			1.2	1.50402	3.772364	19.97024	333.8205	1.510288	2.725605	23.45772
		0.6	1.3	1.959321	5.865176	31.84193	157.4864	2.026237	2.241702	4.578054
			1.4	1.844062	4.860071	20.81439	179.4392	1.459506	1.942673	7.596825
	1.9	0.8	1.5	2.012762	4.86385	14.33673	52.54653	0.812639	1.336533	2.22118
			1.6	1.916656	4.310394	11.52101	37.16466	0.636824	1.287405	2.000305
		0.9	1.7	1.968528	4.461816	11.76748	36.56478	0.586714	1.248579	1.836706
			1.8	1.769355	3.548384	8.136669	21.553	0.417767	1.217309	1.711774

3.3 Moment Generating function for HWIW distribution

Theorem: Let X be a random variable with a pdf is $f(x)$, then MGF of the HWIW distribution is given by:

$$M_x(t) = \sum_{r=0}^{\infty} \frac{t^r}{r!} \left[\frac{\Gamma\left(\frac{n-c}{c}\right)}{cb^{\frac{n-c}{c}}} \left[\frac{M}{(2iu + 2u + j + k)^{\frac{n-c}{c}}} - \frac{N}{(2iu + 2u + j + z)^{\frac{n-c}{c}}} \right] \right]. \tag{3.3}$$

Proof: Let X is a random variable with pdf is $f(x)$, then MGF is given by [16], [17] :

$$M_x(t) = E(e^{tx}) = \int_{-\infty}^{\infty} e^{tx} f(x) dx.$$

Using exponential expansion for above equation, we get a form:

$$M_x(t) = E(e^{tx}) = \sum_{r=0}^{\infty} \frac{t^r}{r!} [\mu_n].$$

From Equation (12), the MGF for HWIW distribution has a from in Equation (3.3).

3.4 Incomplete Moments function for HWIW distribution

Theorem: Let X be a random variable governed by HWIW distribution and $f(x)$ represents its pdf then the incomplete moment function for this distribution is given by:

$$M_n(y) = \frac{M\Gamma\left(\left(\frac{n-c}{c}\right), (2iu+2u+j+k)bx^{-c}\right)}{cb^{\frac{n-c}{c}}(2iu+2u+j+k)^{\frac{n-c}{c}}} - \frac{N\Gamma\left(\left(\frac{n-c}{c}\right), (2iu+2u+j+z)bx^{-c}\right)}{cb^{\frac{n-c}{c}}(2iu+2u+j+z)^{\frac{n-c}{c}}}. \tag{3.4}$$

Proof: assume X is a random variable with pdf is $f(x)$, then the Incomplete Moments function given by the following expression [18]:

$$M_n(y) = \int_{-\infty}^{y} x^n f(x)dx.$$

From Equation (3.2), we get:

$$M_n(y) = \int_0^y x^n\left(Mx^{-(c+1)}e^{-(2iu+2u+j+k)bx^{-c}} - Nx^{-(c+1)}e^{-(2iu+2u+j+z)bx^{-c}}\right)dx,$$

$$M_n(y) = MI_1 - NI_2,$$

where $I_1 = \int_0^y x^{n-(c+1)}e^{-(2iu+2u+j+k)bx^{-c}}\,dx$, and $I_2 = \int_0^y x^{n-(c+1)}e^{-(2iu+2u+j+z)bx^{-c}}\,dx$. For I_1, let $t = (2iu+2u+j+k)bx^{-c}$

$x = \frac{t^{\frac{1}{c}}}{b^{\frac{1}{c}}(2iu+2u+j+k)^{\frac{1}{c}}}$, when $x = 0 \Rightarrow t = 0$ and if $x = y \Rightarrow t = (2iu+2u+j+k)bx^{-c} \Rightarrow dy = \frac{\frac{1}{c}y^{\frac{1}{c}-1}}{b^{\frac{1}{c}}(2iu+2u+j+k)^{\frac{1}{c}}}dt.$

$$I_1 = \int_0^{(2iu+2u+j+k)bx^{-c}} \left(\frac{t^{\frac{1}{c}}}{b^{\frac{1}{c}}(2iu+2u+j+k)^{\frac{1}{c}}}\right)^{n-(c+1)} e^{-t}\frac{y^{\frac{1}{c}-1}}{cb^{\frac{1}{c}}(2iu+2u+j+k)^{\frac{1}{c}}}dt\,,$$

$$I_1 = \frac{\Gamma\left(\left(\frac{n-c}{c}\right),(2iu+2u+j+k)bx^{-c}\right)}{cb^{\frac{n-c}{c}}(2iu+2u+j+k)^{\frac{n-c}{c}}}.$$

Following a similar procedure for I_2 , we arrive at the final form

$$I_2 = \frac{\Gamma\left(\left(\frac{n-c}{c}\right),(2iu+2u+j+z)bx^{-c}\right)}{cb^{\frac{n-c}{c}}(2iu+2u+j+z)^{\frac{n-c}{c}}},$$

then the Incomplete Moments function for HWIW distribution has a from in Equation (3.4).

3.5 Characteristic function of HWIW distribution

Theorem: Let X be a random variable governed by HWIW distribution and $f(x)$ represents its pdf then the Characteristic function for this distribution is given by:

$$Q_x(t) = \sum_{q=0}^{\infty}\frac{(it)^q}{q!}\left[\frac{\Gamma\left(\frac{n-c}{c}\right)}{cb^{\frac{n-c}{c}}}\left[\frac{M}{(2iu+2u+j+k)^{\frac{n-c}{c}}} - \frac{N}{(2iu+2u+j+z)^{\frac{n-c}{c}}}\right]\right]. \tag{3.5}$$

Proof: assume X is a random variable with pdf is $f(x)$, then the Characteristic function given by the following expression [19]:

$$Q_x(t) = E(e^{itx}) = \int_0^{\infty} e^{itx} f(x)\, dx.$$

Using exponential expansion for above equation, then we get a form:

$$Q_x(t) = E(e^{itx}) = \sum_{q=0}^{\infty} \frac{(it)^q}{q!} [\mu_n].$$

From Equation (3.2), the Characteristic function for HWIW distribution has a from in Equation (3.5).

3.6 Rényi entropy for NMWIW distribution

Theorem: Let X be a random variable governed by HWIW distribution and $f(x)$ represents its pdf then the Rényi entropy for this distribution is given by:

$$I_R(r)_{HWIW} = \frac{1}{1-r} \log\left[\theta.\Gamma\left(\frac{1-r(c+1)}{c}\right)\right], \tag{3.6}$$

where $\theta = \sum_{n=0}^{r} (-1)^n \binom{r}{n} M^{r-n} N^n \frac{1}{cb^{\frac{-r(c+1)}{c}+\frac{1}{c}}(2irc+2rc+rj+rk-nk+nz)^{\frac{-r(c+1)}{c}+\frac{1}{c}}}.$

Proof: assume X is a random variable with pdf is $f(x)$, then the Rényi entropy given by the following expression [20]:

$$I_R(c) = \frac{1}{1-c} log \int_0^{\infty} f(x)^c dx.$$

From Equation 10, we get:

$$I_R(r) = \frac{1}{1-r} log \int_0^{\infty} \left(Mx^{-(c+1)} e^{-(2iu+2u+j+k)bx^{-c}} - Nx^{-(c+1)} e^{-(2iu+2u+j+z)bx^{-c}}\right)^r dx.$$

Using the Binomial Series

$$I_R(r) = \frac{1}{1-r} log \int_0^{\infty} \sum_{n=0}^{r} (-1)^n \binom{r}{n} M^{r-n} N^n x^{-r(c+1)}\, e^{-(2irc+2rc+rj+rk-nk+nz)bx^{-c}} dx.$$

$$\text{Let } u = (2irc+2rc+rj+rk-nk+nz)bx^{-c} \Rightarrow x = \frac{u^{\frac{1}{c}}}{b^{\frac{1}{c}}(2irc+2rc+rj+rk-nk+nz)^{\frac{1}{c}}},$$

$$dx = \frac{\frac{1}{c} u^{\frac{1}{c}-1}}{b^{\frac{1}{c}}(2irc+2rc+rj+rk-nk+nz)^{\frac{1}{c}}} du,$$

$$I_R(c)_{HWIW} = \frac{1}{1-r} log = \int_0^{\infty} \sum_{n=0}^{r} (-1)^n \binom{r}{n} M^{r-n} N^n \left(\frac{u^{\frac{1}{c}}}{b^{\frac{1}{c}}(2irc+2rc+rj+rk-nk+nz)^{\frac{1}{c}}}\right)^{-r(c+1)},$$

$$e^{-u}\frac{\frac{1}{c}u^{\frac{1}{c}-1}}{b^{\frac{1}{c}}(2irc+2rc+rj+rk-nk+nz)^{\frac{1}{c}}}du.$$

Put $\theta=\sum_{n=0}^{r}(-1)^n\binom{r}{n}M^{r-n}N^n\frac{1}{cb^{\frac{-r(c+1)}{c}+\frac{1}{c}}(2irc+2rc+rj+rk-nk+nz)^{\frac{-r(c+1)}{c}+\frac{1}{c}}}$,

$$I_R(r)_{HWIW}=\frac{1}{1-r}\log\left[\theta\int_0^\infty u^{\frac{-r(c+1)}{c}+\frac{1}{c}-1}e^{-u}du\right],$$

$$I_R(r)_{HWIW}=\frac{1}{1-r}\log\left[\theta.\Gamma\left(\frac{1-r(c+1)}{c}\right)\right].$$

Then the Rényi entropy for HWIW distribution has a from in Equation (3.6).

4. Estimation

4.1 Maximum likelihood estimation (MLE)

The estimation of HWIW distribution parameters is carried out using the MLE. Consider that the random variable follows the HWIW$(r,u,b.c)$, and the parameter vector is denoted by $\Delta=(r,u,b,c)^T$, the log-likelihood function corresponding to Δ is expressed as [21], [22]:

$$L(\theta,x_i)=\prod_{i=1}^{m}\quad rubcx^{-(c+1)}e^{-bx^{-c}}\left[\frac{e^{-bx^{-c}}}{1-e^{-bx^{-}}}-log\left(1-e^{-bx^{-c}}\right)\right]$$

$$\times\left[-e^{-bx^{-c}}.log\left(1-e^{-bx^{-c}}\right)\right]^{u-1}e^{\left(-r\left[-e^{-bx^{-c}}.log\left(1-e^{-bx^{-c}}\right)\right]^{u}\right)}$$

we compute the log- likelihood:

$$l=l(\Delta)=mlog(r)+mlog(u)+mlog(b)+mlog(c)-(c-1)\sum_{i=1}^{m}\log(x_i)-\sum_{i=1}^{m}bx_i^{-c}$$

$$+\sum_{i=1}^{m}\log\left[\frac{e^{-bx_i^{-c}}}{1-e^{-bx_i^{-c}}}-log\left(1-e^{-bx_i^{-c}}\right)\right]+(u-1)\sum_{i=1}^{m}\log\left[-e^{-bx_i^{-c}}.log\left(1-e^{-bx_i^{-c}}\right)\right] \tag{4.1}$$

$$-r\sum_{i=1}^{m}\left[-e^{-bx_i^{-c}}.log\left(1-e^{-bx_i^{-c}}\right)\right]^{u}.$$

4.2 Least square estimation

The Least square estimation (LSE) method can be used to estimate a parameter using the following formula [23]:

$$\varphi(\theta_N)=\sum_{i=1}^{m}\left[1-e^{\left(-r\left[-e^{-bx^{-c}}.\log\left(1-e^{-bx^{-c}}\right)\right]^{u}\right)}-\frac{i}{n+1}\right]^2. \tag{4.2}$$

4.3 Weighted Least square estimation (WLSE)

Parameter can be estimated using the WLSE technique through the following expression [24]:

$$W(\theta_N) = \sum_{i=1}^{m} \frac{(n+1)^2(n+2)}{i(n-i+1)} \left[1 - e^{\left(-r\left[-e^{-bx^{-c}}.log\left(1-e^{-bx^{-c}}\right)\right]^u\right)} - \frac{i}{n+1}\right]^2. \qquad (4.3)$$

Parameter estimates are derived using the three methods mentioned above, by partially differentiating the likelihood function for the four parameters and then setting the derivatives equal to zero. Given the complexity of numerical solutions to these equations, computational techniques such as the R language are used to obtain the desired values.

5. Simulation

Monte Carlo simulation is a mathematical technique that relies on random variables to model complex systems and analyze their behavior. It is widely applied in statistics, economics, engineering, and the natural sciences because of its ability to yield accurate estimates for models whose solutions are difficult or even impossible to obtain with traditional analytical methods. The core idea is to generate a large number of random samples in order to compute specific quantities or estimate probabilistic outcomes, thereby facilitating the study of phenomena that are hard to predict analytically. To assess the efficiency and accuracy of estimating the parameters of the HWIW distribution, a Monte Carlo simulation was carried out using the three estimation methods: MLE, LSE, WLSE. Random samples of sizes $\mathrm{n} = 50{,}100{,}150{,}200{,}250$ and up to $n = 1000$ ere generated, and the performance of each method was evaluated with respect to three criteria MSE, RMSE [25], [26], and Bias of the parameter estimates.

The simulation results are summarized in Table 3, which reports all three performance measures for each sample size, providing a practical evaluation of the effectiveness of the estimation techniques.

Table 3: Results of Monte Carlo simulations applied to the HWIW distribution.

$\boldsymbol{r = 0.6}$, $\boldsymbol{u = 0.9}$, $\boldsymbol{b = 0.7}$, $\boldsymbol{c = 1.2}$					
N	**Est.**	**Ess. Par.**	**MLE**	**LSE**	**WLSE**
50	**Mean**	$\hat{\boldsymbol{r}}$	0.66218994	0.7935073	0.7945322
		$\hat{\boldsymbol{u}}$	0.94482752	0.90725405	0.87221447
		$\hat{\boldsymbol{b}}$	0.8173529	0.9586352	0.9458078
		$\hat{\boldsymbol{c}}$	1.6005334	1.3007755	1.3224457
	MSE	$\hat{\boldsymbol{r}}$	0.34450955	0.3029998	0.3196053
		$\hat{\boldsymbol{u}}$	0.09171262	0.16296775	0.09943654
		$\hat{\boldsymbol{b}}$	0.5872540	0.5312079	0.5426379
		$\hat{\boldsymbol{c}}$	0.8883328	0.4236644	0.3828196

	RMSE	$\hat{r}$	0.58694936	0.5504542	0.5653365
		$\hat{u}$	0.30284092	0.40369264	0.31533560
		$\hat{b}$	0.7663250	0.7288401	0.7366396
		$\hat{c}$	0.9425141	0.6508951	0.6187241
	Bias	$\hat{r}$	0.06218994	0.1935073	0.1945322
		$\hat{u}$	0.04482752	0.00725405	0.02778553
		$\hat{b}$	0.1173529	0.2586352	0.02778553
		$\hat{c}$	0.4005334	0.1007755	0.1224457
100	**Mean**	$\hat{r}$	0.64384318	0.7219438	0.7182429
		$\hat{u}$	0.94033751	0.87454167	0.87775399
		$\hat{b}$	0.76723431	0.8778392	0.8340620
		$\hat{c}$	1.4001384	1.3028549	1.27703038
	MSE	$\hat{r}$	0.23499950	0.2124502	0.1981540
		$\hat{u}$	0.06256473	0.07460193	0.04674475
		$\hat{b}$	0.33109832	0.3405407	0.2714449
		$\hat{c}$	0.2971453	0.2258667	0.18424882
	RMSE	$\hat{r}$	0.48476747	0.4609232	0.4451449
		$\hat{u}$	0.25012943	0.27313355	0.21620533
		$\hat{b}$	0.57541144	0.5835586	0.5210037
		$\hat{c}$	0.5451103	0.4752543	0.42924215
	Bias	$\hat{r}$	0.5451103	0.1219438	0.1182429
		$\hat{u}$	0.04033751	0.02545833	0.02224601
		$\hat{b}$	0.06723431	0.1778392	0.1340620
		$\hat{c}$	0.2001384	0.1028549	0.07703038

150	Mean	$\hat{r}$	0.609999358	0.7218282	0.64903158
		$\hat{u}$	0.95149716	0.87361891	0.91132615
		$\hat{b}$	0.72423747	0.8539909	0.75548383
		$\hat{c}$	1.3746361	1.27230291	0.75548383
	MSE	$\hat{r}$	0.180700778	0.2093021	0.16223096
		$\hat{u}$	0.05561927	0.05271935	0.04119156
		$\hat{b}$	0.25410926	0.2817639	0.20157287
		$\hat{c}$	0.2018948	0.13858398	0.1762926
	RMSE	$\hat{r}$	0.425089141	0.4574955	0.40277904
		$\hat{u}$	0.23583739	0.22960694	0.20295704
		$\hat{b}$	0.50409251	0.5308143	0.44896867
		$\hat{c}$	0.4493271	0.37226869	0.4198721
	Bias	$\hat{r}$	0.009999358	0.1218282	0.04903158
		$\hat{u}$	0.05149716	0.02638109	0.01132615
		$\hat{b}$	0.02423747	0.1539909	0.05548383
		$\hat{c}$	0.1746361	0.07230291	0.1213862
	Mean	$\hat{r}$	0.62953303	0.67330833	0.62552888
		$\hat{u}$	0.92401550	0.892643858	0.91648996
		$\hat{b}$	0.73728692	0.8049638	0.7284962
		$\hat{c}$	1.3183908	1.25742869	1.3022389
	MSE	$\hat{r}$	0.14542449	0.12782454	0.12441776
		$\hat{u}$	0.03766835	0.043226750	0.03072519
		$\hat{b}$	0.18643346	0.2099843	0.1550041
		$\hat{c}$	0.1322101	0.11526679	0.1274526

200	**RMSE**	$\hat{r}$	0.38134563	0.3636071	0.35272902
		$\hat{u}$	0.19408336	0.207910437	0.17528603
		$\hat{b}$	0.43177941	0.4582404	0.3937056
		$\hat{c}$	0.3636071	0.33950963	0.3570051
	Bias	$\hat{r}$	0.02953303	0.07330833	0.02552888
		$\hat{u}$	0.02401550	0.007356142	0.01648996
		$\hat{b}$	0.03728692	0.1049638	0.0284962
		$\hat{c}$	0.1183908	0.05742869	0.1022389
250	**Mean**	$\hat{r}$	0.605497333	0.67616917	0.608383893
		$\hat{u}$	0.93281004	0.88124099	0.92341073
		$\hat{b}$	0.706005227	0.79824836	0.71403583
		$\hat{c}$	1.30557693	1.26590402	1.29949605
	MSE	$\hat{r}$	0.109527538	0.12320369	0.108918047
		$\hat{u}$	0.03389573	0.03761672	0.03328868
		$\hat{b}$	0.136416881	0.17672820	0.14360899
		$\hat{c}$	0.09854788	0.10182472	0.10257126
	RMSE	$\hat{r}$	0.330949450	0.35100383	0.330027342
		$\hat{u}$	0.18410793	0.19395029	0.18245186
		$\hat{b}$	0.369346559	0.42039054	0.37895777
		$\hat{c}$	0.31392336	0.31909986	0.32026748
	Bias	$\hat{r}$	0.005497333	0.07616917	0.008383893
		$\hat{u}$	0.03281004	0.01875901	0.02341073
		$\hat{b}$	0.006005227	0.09824836	0.01403583
		$\hat{c}$	0.10557693	0.06590402	0.09949605

Table 3 Display the outcomes of a Monte Carlo simulation used to estimate the parameters of the HWIW distribution through three distinct estimation techniques: (MLE, LSE, and WLSE). The table shows that the estimation accuracy improves with increasing sample size, with both MSE and RMSE values gradually decreasing from 50 to 250 sample size. The results show that the WLES method performs best in terms of accuracy for most parameters, especially for small and medium sample sizes, while the MLE method maintained the lowest Bias values in most cases, indicating its stability and reliability.

The LSE method, on the other hand, performed relatively poorly, particularly in accurately estimating parameters at small sample size, with higher MSE and Bias values. These results reflect the importance of choosing the appropriate estimation method based on sample size and statistical accuracy requirements.

6. Application

To demonstrate the robustness and applicability of the proposed distribution in real-world contexts, the practical component plays a central role in this evaluation. Therefore, this section provides a real-data application, accompanied by and benchmarked against six established distributions for performance assessment

- Beta with baseline inverse Weibull (BeIW)
- Kumaraswamy with baseline inverse Weibull (KuIW)
- Exponeted generalized with baseline inverse Weibull (EGIW)
- Log-Gamma with baseline inverse Weibull (LGamIW)
- Gompertz with baseline inverse Weibull (GoIW)
- Inverse Wiebull (IW)

All of the selected distribution belongs to extended or modified families of the IW distribution, making them direct competitors of the HWIW distribution. These distributions serve as powerful models for statistical data analysis, and the HWIW distribution stands among them due to its flexibility and ability to accurately represent data, which was the primary motivation behind its development. This comparison was conducted using four informative criteria AIC [27], CAIC [28], BIC [29], and HQIC [30]. Four statistical measures were also used to evaluate accuracy K-S, A, W and p-value.

Data set-1: The dataset used in this study includes the survival times of 72 guinea pigs that were infected with virulent tubercle bacilli. The survival times are measured in days. The original observation and reporting of this dataset were conducted by Bjerkedal [5].

0.1, 0.33, 0.44, 0.56, 0.59, 0.59, 0.72, 0.74, 0.92, 0.93, 0.96, 1, 1, 1.02, 1.05, 1.07, 1.07, 1.08, 1.08, 1.08, 1.09, 1.12, 1.13, 1.15, 1.16, 1.2, 1.21, 1.22, 1.22, 1.24, 1.3, 1.34, 1.36, 1.39, 1.44, 1.46, 1.53, 1.59, 1.6, 1.63, 1.63, 1.68, 1.71, 1.72, 1.76, 1.83, 1.95, 1.96, 1.97, 2.02, 2.13, 2.15, 2.16, 2.22, 2.3, 2.31, 2.4, 2.45, 2.51, 2.53, 2.54, 2.54, 2.78, 2.93, 3.27, 3.42, 3.47, 3.61, 4.02, 4.32, 4.58 , 5.55.

Table 4 provides a summary of the model selection criteria used to compare the distribution. Table 5 reports the corresponding statistical test values, while Table 6 displays the estimated parameters for each distribution under study.

Table 4. results of the criteria for the distributions.

Dist.	-log	AIC	CAIC	BIC	HQIC
HWIW	95.88984	199.8247	200.4217	208.9313	203.4501
BeIW	101.296	210.6642	211.2612	219.7708	214.2895
KuIW	97.89873	203.7986	204.3956	212.9053	207.424
EGIW	100.9368	209.8826	210.4796	218.9893	213.508
LGamIW	99.80569	207.6247	208.2217	216.7314	211.2501
GoIW	97.17087	202.3418	202.9388	211.4485	205.9672
IW	118.1178	240.2356	240.4095	244.7889	242.0483

Table 4 shows the results of the comparison criteria between the distributions, with lower values indicating better performance. The evaluation results showed that the HWIW distribution achieved the lowest values across all criteria (AIC, BIC, etc.), demonstrating its superior representation of the data. In contrast, the IW distribution achieved the highest values, indicating its poor fit compared to the other distributions.

Table 5. value of the statistical measures.

Dist.	W	A	K-S	p-value
HWIW	0.0922143	0.6110752	0.1130676	0.316085
BeIW	0.1675262	1.155408	0.1438356	0.1016569
KuIW	0.1107239	0.7703783	0.11985	0.2522606
EGIW	0.1608632	1.111592	0.1402135	0.117882
LGamIW	21.91134	141.258	0.9999952	5.797307e-63
GoIW	0.1616563	0.9825052	0.1283847	0.1861575
IW	0.5284354	3.310617	0.1991304	0.006625223

Table 5 shows the results of the statistical goodness-of-fit measures. Lower values for W, A, and K-S indicate a better fit to the data, and p-values are an additional indicator of this. The HWIW distribution performed best, achieving the lowest values across all measures and the highest p-value (0.316), indicating a strong fit to the data. In contrast, distributions such as LGamIW and IW performed poorly, with high values and very low p-values, indicating poor representativeness of the data.

Table 6. Estimator value interval for parameters by MLE.

Dist.	$\hat{r}_N$	$\hat{u}_N$	$\hat{b}_N$	$\hat{c}_N$
HWIW	1.3782752	3.1107381	0.4686840	0.5414699
BeIW	0.9168564	5.9240884	3.0074058	0.7257823
KuIW	2.0448702	15.6432752	1.9116895	0.5584649
EGIW	6.5028232	0.9572174	3.0215673	0.7065691
LGamIW	0.6738629	7.9310308	3.9767690	0.7099198
GoIW	0.7349332	3.2243297	1.4417615	0.6936903
IW	----	-----	1.061440	1.171994

Table 6 displays parameter estimates for the distributions using the MLE. The HWIW distribution showed moderate parameters, reflecting a good balance of representativeness. In contrast, distributions such as KuIW and EGIW recorded high values for some parameters, indicating more complex models. The IW distribution, being simpler than the other distributions, contained only two parameters. These estimates reflect the flexibility of each distribution in representing data.

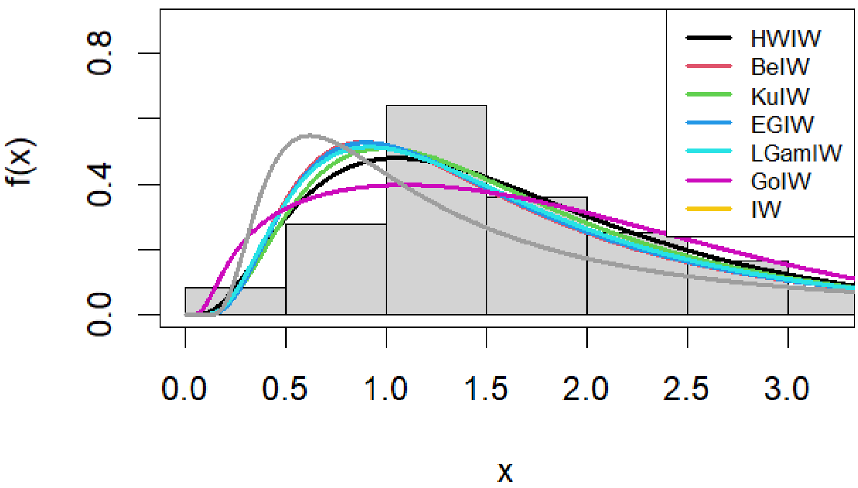

Figure 5: Fitting PDFs HWIW with histogram data set.

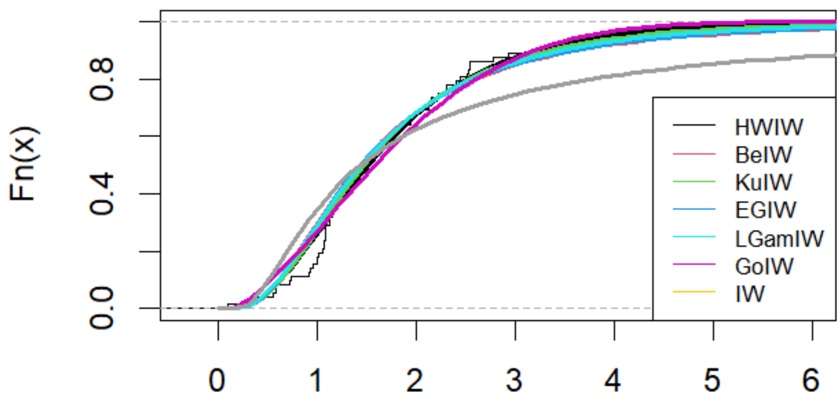

Figure 6: Empirical Fitted CDFs HWIW with data set.

Figure 5 displays how well the pdf of the WHIW distribution aligns with the first dataset. The fitted curve demonstrates a close match to the empirical data, effectively capturing its structural characteristics, reflecting the high efficiency of the HWIW distribution in efficiently and flexibly representing the actual behavior of the data.Figure 6 shows a comparison between the empirical CDF and the theoretical cumulative distribution associated with the HWIW distribution. This figure shows a clear fit between the two curves, confirming the proposed distribution's ability to accurately represent the cumulative probability of the data, thus reflecting its effectiveness in reliably modeling real data.

Data set-2: Failure Times of 50 Components [29]

0.036, 0.058, 0.061, 0.074, 0.078, 0.086, 0.102, 0.103, 0.114, 0.116, 0.148, 0.183, 0.192, 0.254, 0.262, 0.379, 0.381, 0.538, 0.570, 0.574, 0.590, 0.618, 0.645, 0.961, 1.228, 1.600, 2.006, 2.054, 2.804, 3.058, 3.076, 3.147, 3.625, 3.704, 3.931, 4.073, 4.393, 4.534, 4.893, 6.274,6.816, 7.896, 7.904, 8.022, 9.337, 10.940, 11.020, 13.880, 14.730, 15.080

Table 7. results of the criteria for the distributions.

Dist.	**-log**	**AIC**	**CAIC**	**BIC**	**HQIC**
HWIW	102.5897	213.1842	214.0731	220.8323	216.0967
BeIW	104.7622	217.5404	218.4292	225.1884	220.4528
KuIW	104.4104	216.8386	217.7275	224.4867	219.7511
EGIW	104.7671	217.5438	218.4327	225.1919	220.4562
LGamIW	104.4651	217.0186	217.9075	224.6667	219.931
GoIW	104.5873	217.1846	218.0735	224.8327	220.0971
IW	106.0967	216.1933	216.4486	220.0174	217.6495

Table 7 shows that the HWIW distribution achieved the lowest values across all information metrics (AIC, BIC, CAIC, and HQIC) compared to the other distributions, demonstrating its high data-fitting efficiency. In contrast, distributions such as BeIW, GoIW, and EGIW achieved higher values, reflecting their poor performance compared to HWIW.

Table 8. value of the statistical measures.

Dist.	W	A	K-S	p-value
HWIW	0.1719594	1.063281	0.1379881	0.2711381
BeIW	0.2246938	1.384528	0.1585079	0.1453208
KuIW	0.2160847	1.333744	0.1558378	0.1584046
EGIW	0.224653	1.384445	0.1614739	0.1318197
LGamIW	17.95769	99.77021	0.9818669	8.881784e-16
GoIW	0.2123711	1.31562	0.1496055	0.1925845
IW	0.2575837	1.57173	0.16011	0.1378965

Table 8 shows that the HWIW distribution performed best among the compared distributions, recording the lowest values for the W, A, and K-S metrics, along with the highest p-value, confirming its accurate representation of the data. In contrast, distributions such as IW and LGamIW performed poorly, indicating their poor fit to the data.

Table 9. Estimator value interval for parameters by MLE.

Dist.	$\hat{r}_N$	$\hat{u}_N$	$\hat{b}_N$	$\hat{c}_N$
HWIW	1.2975383	2.5187226	0.3953556	0.2346634
BeIW	1.2809056	2.1997463	1.0261864	0.3948558
KuIW	1.3911669	2.7407636	1.0465352	0.3649795
EGIW	2.1705086	1.0785869	1.1698675	0.4009732
LGamIW	1.2129747	2.9472049	1.3521062	0.3473045
GoIW	1.2129747	2.9472049	1.3521062	0.3473045
IW	----	-----	0.6040943	0.5912884

Table 9 shows that the HWIW distribution provided more stable and accurate parameter estimates than the other distributions. However, distributions such as GoIW and BeIW exhibited significant variability in estimates, indicating their low reliability.

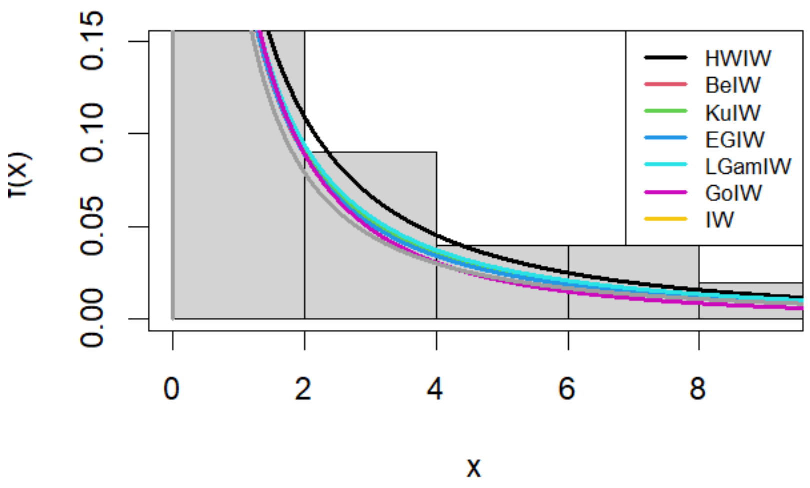

Figure 7: Fitting PDFs HWIW with histogram data set-II.

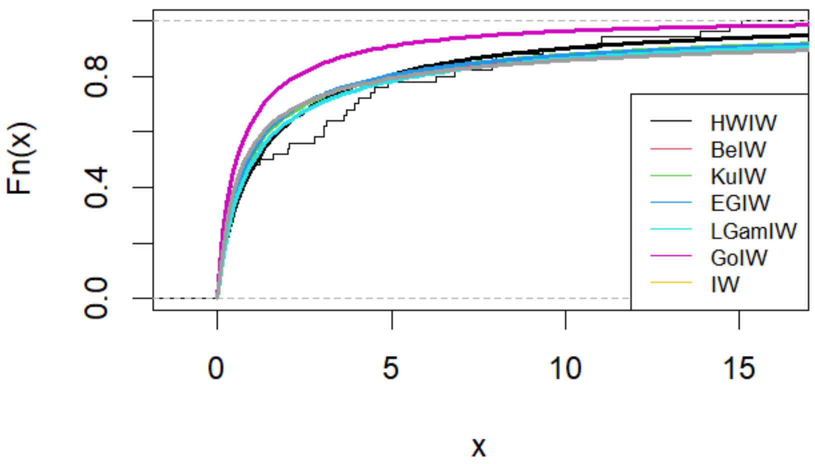

Figure 8: Empirical Fitted CDFs HWIW with data set-II.

Figure 7 highlights the extent to which the PDF of the HWIW distribution matches the histogram of the experimental data. This distribution clearly demonstrates its ability to represent the overall shape of the data, especially in the early regions of the distribution and the slope, reflecting the flexibility of the HWIW in accommodating variations and the actual behavior of the data. Figure 8 shows a close convergence between the theoretical CDF of the HWIW distribution and the experimental cumulative distribution. This convergence supports the model's ability to accurately represent the cumulative behavior of the data, even in the presence of variability or uncertainty in the experimental values.

7. Conclusion

The HWIW distribution demonstrated high efficiency in representing complex real-world data, clearly outperforming six competing extended IW distributions. It achieved the lowest information criterion value (AIC, CAIC, BIC, HQIC), the best goodness of fit indices (W, A, K-S), and the highest likelihood value (P-value), reflecting its accurate and effective modeling capabilities. The results confirmed the HWIW distribution's adaptability to asymmetric and heavy-tailed data, making it well-suited for representing a wide range of real-world datasets. Monte-Carlo simulation results revealed that the WLSE method was the most accurate in terms of MSE and RMSE, particularly for small and medium-size samples, while the MLE method exhibited lower bias and greater stability as sample size increased. In contrast, the LES method performed relatively poorly, underscoring the importance of selecting the appropriate estimation method based on sample size and analysis goals-WLES for accuracy and MLE for stable. The proposed distribution possesses advanced mathematical properties, such as the flexibility of density and distribution functions, and the ease of deriving moments, quantile function, and entropy, enhancing its reliability as an analytical tool in applied statistics. Given its superiority over other distributions, the HWIW is a promising model that can be extended to multidimensional data or combined with artificial intelligence and machine learning techniques to improve predictions in uncertain environments. These results open new avenues for employing the HWIW distribution in a wide range of real-world applications, including medical, industrial, and social fields, where traditional models present challenges in representing variance and skewness in real data.

Authors' Contributions:

Authors have worked equally to write and review the manuscript.

Data Availability Statement:

The data that supports the findings of this study are available within the article.

Conflicts of Interest:

The authors declare no conflict of interest.

References

[1] Alzaatreh, A., Lee, C., and Famoye, F. (2013). A new method for generating families of continuous distributions. *Metron*, 71(1), 63-79.

[2] Hussain, S., Hassan, M. U., Rashid, M. S., and Ahmed, R. (2023). Families of Extended Exponentiated Generalized Distributions and Applications of Medical Data Using Burr III Extended Exponentiated Weibull Distribution. *Mathematics*, 14(11), 3090.

[3] Odeyale, A. B., Gulumbe, S. U., Umar, U., and Aremu, K. O. (2023). New Odd Generalized Exponentiated Exponential-G Family of Distributions. *UMYU Scientifica*, 4(2), 56-64.

[4] Noori, N. A., Khalaf, A. A., and Khaleel, M. A. (2023). A New Generalized Family of Odd Lomax-G Distributions Properties and Applications. *Advances in the Theory of Nonlinear Analysis and Its Application*, 4(7), 1-16.

[5] Sadiq, I. A., Doguwa, S. I., Yahaya, A., and Garba, J. (2023). New Generalized Odd Fréchet-G (NGOF-G) Family of Distribution with Statistical Properties and Applications. *UMYU Scientifica*, 3(2), 100-107.

[6] Abdelall, Y. Y., Hassan, A. S., and Almetwally, E. M. (2024). A new extension of the odd inverse Weibull-G family of distributions: Bayesian and non-Bayesian estimation with engineering applications. *Computational Journal of Mathematical and Statistical Sciences*, 2(3), 359-388.

[7] Ishaq, A. I., Panitanarak, U., Alfred, A. A., Suleiman, A. A., and Daud, H. (2024). The Generalized Odd Maxwell-Kumaraswamy Distribution: Its Properties and Applications. *Contemporary Mathematics*, 1(1), 711-742.

[8] Noori, N. A., Abdullah, K. N., and Khaleel, M. A. (2025). Data Modelling and Analysis Using Odd Lomax Generalized Exponential Distribution: an Empirical Study and Simulation. *Iraqi Statisticians Journal*, 1(2), 146-162.

[9] Mahdi, G. A., Khaleel, M. A., Gemeay, A. M., Nagy, M., Mansi, A. H., Hossain, M. M., and Hussam, E. (2024). A new hybrid odd exponential-Φ family: Properties and applications. *AIP Advances*, 14(4), 1-15.

[10] Noori, N. A., and Khaleel, M. A. (2024). Estimation and Some Statistical Properties of the hybrid Weibull Inverse Burr Type X Distribution with Application to Cancer Patient Data. *Iraqi Statisticians Journal*, 2(1), 8-29.

[11] Noori, N. A., Khalaf, A. A., and Khaleel, M. A. (2024). A new expansion of the Inverse Weibull Distribution: Properties with Applications. *Iraqi Statisticians Journal*, 1(1), 52-62.

[12] Noori, N. A. (2023). Exploring the Properties, Simulation, and Applications of the Odd Burr XII Gompertz Distribution. *Advances in the Theory of Nonlinear Analysis and Its Application*, 4(7), 60-75.

[13] Khalaf, A. A., Khaleel, M. A., and Noori, N. A. (2024). A new expansion of the Inverse Weibull Distribution: Properties with Applications. *Iraqi Statisticians Journal*, 1(1), 52-62.

[14] Alanaz, M. M., and Algamal, Z. Y. (2023). Neutrosophic exponentiated inverse Rayleigh distribution: Properties and Applications. *International Journal of Neutrosophic Science*, 21(4), 36-43.
[15] Khalaf, A. A., Ibrahim, M. Q., and Noori, N. A. (2024). [0,1] Truncated Exponentiated Exponential Burr type X Distribution with Applications. *Iraqi Journal of Science*, 65(8), 4428-4440.
[16] Gómez, H. J., Santoro, K. I., Chamorro, I. B., Venegas, O., Gallardo, D. I., and Gómez, H. W. (2023). A Family of Truncated Positive Distributions. *Mathematics*, 11(21), 4431.
[17] Muhammad, B., Mohsin, M., and Aslam, M. (2021). Weibull-exponential distribution and its application in monitoring industrial process. *Mathematical Problems in Engineering*, 2021(1), 1-13.
[18] Al Abbasi, J. N., Resen, I. A., Abdulwahab, A. M., Oguntunde, P. E., Al-Mofleh, H., and Khaleel, M. A. (2023). The right truncated Xgamma-G family of distributions: Statistical properties and applications. *AIP Conference Proceedings*, 2834(1), 1-15.
[19] Al-Habib, K. H., Khaleel, M. A., and Al-Mofleh, H. (2023). A new family of truncated Nadarajah-Haghighi-G properties with real data applications. *Tikrit Journal of Administrative and Economic Sciences*, 19(61), 2.
[20] Afify, A. Z., Yousof, H., and Nadarajah, S. (2017). The beta transmuted-H family for lifetime data. *Statistics and its Interface*, 10(3), 505-520.
[21] Bhatti, F. A., Hamedani, G. G., Korkmaz, M. C., Cordeiro, G. M., Yousof, H. M., and Ahmad, M. (2019). On Burr III Marshal Olkin family: development, properties, characterizations and applications. *Journal of Statistical Distributions and Applications*, 6(1), 1-21.
[22] Teamah, A.-E. A. M., Elbanna, A. A., and Gemeay, A. M. (2020). Frèchet-Weibull distribution with applications to earthquakes data sets. *Pakistan Journal of Statistics*, 36(2), 135-147.
[23] Abd El-latif, A. M., Almulhim, F. A., Noori, N. A., Khaleel, M. A., and Alsaedi, B. S. (2025). Properties with application to medical data for new inverse Rayleigh distribution utilizing neutrosophic logic. *Journal of Radiation Research and Applied Sciences*, 18(2), 101391.
[24] Abed, R. A., Khaleel, M. A., and Noori, N. A. (2025). Modified Weibull-Fréchet Distribution Properties with Application. *Iraqi Statisticians Journal*, 1(2), 195-216.
[25] Noori, N. A., Ahmed, D. D., and Khaleel, M. A. (2025). Odd Lomax Chen distribution: An Innovative Statistical Tool for Improving Real Data Modeling and Its Practical Applications. *Tikrit Journal of Administrative and Economic Sciences*, 21(Special Issue, Part 1), 1098-1126.
[26] Noori, N. A., Khaleel, M. A., and Salih, A. M. (2025). Some Expansions to The Weibull Distribution Families with Two Parameters: A Review. *Babylonian Journal of Mathematics*, 1(1), 61-87.
[27] Noori, N. A., Khaleel, M. A., Khalaf, S. A., and Dutta, S. (2025). Analytical Modeling of Expansion for Odd Lomax Generalized Exponential Distribution in Framework of Neutrosophic Logic: a Theoretical and Applied on Neutrosophic Data. *Innovation in Statistics and Probability*, 1(1), 47-59.
[28] Habib, K. H., Khaleel, M. A., Al-Mofleh, H., Oguntunde, P. E., and Adeyeye, S. J. (2024). Parameters Estimation for the [0, 1] Truncated Nadarajah Haghighi Rayleigh Distribution. *Scientific African*, 1(1), e02105.
[29] Khaoula, A., Seddik-Ameur, N., Abd El-Baset, A. A., and Khaleel, M. A. (2022). The Topp-Leone Extended Exponential Distribution: Estimation Methods and Applications. *Pakistan Journal of Statistics and Operation Research*, 18(4), 817-836